Korean J. Chem. Eng., **22**(2), 285-290 (2005)

Polypyrrole Composite Membrane with High Permeability Prepared by Interfacial Polymerization

Won-Il Son, Jae-Min Hong* and Byoung-Sik Kim†

Department of Chemical Engineering, Dongguk University, Pil-dong, Chung-gu, Seoul 100-715, Korea
*Optoelectronic Materials Center, Korea Institute of Science and Technology, P.O box 131, Cheongryang, Seoul 130-650, Korea
(*Received 26 November 2004 • accepted 20 December 2004*)

Abstract–Novel polypyrrole (PPy)/polydimethylsiloxane (PDMS) composite membrane was prepared by interfacial polymerization to make a very effective gas separation membrane. We found that Polymerized PPy films as thin as ~200 nm could be chemically synthesized as freestanding membranes by using the interfacial polymerization technique. Additionally, we show that difference morphology of PPys films was obtained by controlling polymerization rate and more dense films were formed at low polymerization rate. Wide X-ray diffraction study showed the d spacing value of the PPy film decreased from 4.89 Å to 3.67 Å by the rate of polymerization decreases. According to d spacing value decrease, selectivity of a PPy composite membrane was increased dramatically and permeability was reduced gradually. This high selectivity was derived from d spacing closed to the kinetic diameter of nitrogen. These results indicated that the permeability is controlled by the diffusion coefficient, reflecting the packed structure of the PPy film. The highest selectivity value of composite membrane that was prepared by interfacial polymerization was O_2/N_2=17.2 and permeability for O_2 was 40.2 barrer.

Key words: Polypyrrole, Interfacial Polymerization, Gas Separation, Ultra-thin

INTRODUCTION

Gas separation membrane technology is useful for a variety of applications [Henis et al., 1980; Abelson et al., 1989], such as hydrogen recovery from reactor purge gas, nitrogen and oxygen enrichment, water vapor removal from air, stripping of carbon dioxide from natural gas, etc. Although membrane separations are attractive because of low energy costs and simple operation, low permeabilities and/or selectivities often limit membrane applications [Spillman, 1989; Haggin, 1990]. Gas separation membrane requires simultaneously high permeability and high permselectivity for practical use. These quantities for typical polymers, generally, show a reverse relationship; polymers with high permeabilities show low permselectivity and polymers with high permselectivity show low permeabilities. To overcome these limitations many researchers have attempted to make increasing efficient surface area of membrane or/and decreasing thickness of selectivity layer vital for increasing flux without sacrificing selectivity. Current strategies for improving gas flux are largely directed towards reducing the skin thickness of the membrane, i.e., asymmetric or composite membrane. The asymmetric membrane has a thin, dense layer on the surface of a more porous substructured layer. And the composite membrane has a dense skin layer supported on a porous layer, two layers being composed of different polymers. The dense skin layers of the membranes are responsible for the separation and also allow high fluxes due to tie thinness. However, the number of polymers that can be prepared in an asymmetric form is limited and the preparation of the composite membrane involves many technical problems [Spillman, 1989].

To overcome those limitations and technical problems, we have attempted to decrease thickness of the selectivity layer vital for increasing flux without sacrificing selectivity. This study used PPy as selective layer and PDMS as support layer due to very high gas permeability efficiencies. PPy films prepared by interfacial polymerization are ultra-thin and adhesive well to a PDMS as support layer. In order to understand, the morphology of prepared membranes has been carried out by scanning electron microscope (SEM). The polymerized PPy films were characterized by FT-IR and wide-angle X-ray diffraction (WAXD). Thermogravimetry (TGA) was carried out on a thermogravimetric analyzer.

EXPERIMENTS

1. Materials

Pyrrole monomer was purchased from Aldrich Chemicals and vacuum distilled prior to use. The present work was carried out in aqueous solutions (millim Q water) and *n*-hexane as a organic solution. The aqueous solutions of ferric chloride ($FeCl_3$, Wako) and ferrous chloride ($FeCl_2$, Aldrich) were used with filtration (pore size 0.05 μm).

2. Preparation of Composite Membrane

Flat PPy/PDMS composite membranes were prepared by interfacial polymerization methods. Interfacial synthesis was performed by putting a 30 ml aqueous solution of ferrous chloride (0.4 M) and ferric chloride (0.5 M) as oxidation agents into Petri-dish (87×15 mm). Pyrrole monomer in the non-aqueous phase (*n*-hexane) was poured slowly on the oxidizing agent in the aqueous phase. The PPy monomer and the oxidants reagent diffuse towards each other to yield a thin polypyrrole film at the interface between the two immiscible phases. A glass slide, acting as a substrate, was placed just

†To whom correspondence should be addressed.
E-mail: bskim@dongguk.edu
‡This paper is dedicated to Professor Woo Sik Kim on the occasion of his retirement from Yonsei University

below the interface. Within a few minutes, a thin film started to appear at the interface. After given polymerization time, we removed the solutions in the interfacial at over and below. Then the polymerized PPy film was placed on a glass slide; smooth and compact films could be obtained in a reproducible manner. After polymerization, the polymerized PPy film was rinsed by methanol to remove excess monomer and oxidizing agent. Composite membranes were prepared by simply pouring a solution of PDMS in n-hexane on the surface of polymerized PPy film on the placed glass slide. After PDMS was cured for 24 hours, composite membrane was annealed in air at 80 °C for 15 min. Prepared composite membranes were carefully removed from the surface of the glass plate by simply washing with water. Final thickness of the prepared PPy/PDMS composite membranes obtained was between about 200 and 300 μm.

3. Gas Permeability Measurements

The gas transport cell is described elsewhere [Lee et al., 1999]. Membrane samples were prepared by sandwiching the composite membrane between aluminum foil tape (All-foil. Inc.). A circular hole was punched into the aluminum foil tape; this hole defines the area of the membrane exposed to permeate gas. Epoxy was applied at the interface of the tape and the composite membrane to prevent any gas leak. The gas permeation measurements of the membranes were carried out at 35 °C.

Permeation experiments were realized by using the constant volume and variable pressure technique in a permeability apparatus at constant temperature (298 K). The system consisted essentially on a permeation cell with two compartments separated by the tested membrane. Before each experiment the system was strongly outgased during 48 h at high vacuum (1.0×10^{-5} torr) using a turbomolecular pump (Leybold, Turbovac 50) in downstream. The permeability experiments were performed by using around 200 torr of upstream pressure and recording the pressure increase in the downstream compartment by a pressure transducer, and pressure increases on the permeate side versus time data were recorded by a computer. The purity of gases used (O_2 and N_2) was of 99.95%; they were used without any further purification. For every gas, measurements were repeated twice after re-evacuation of chambers and degasification of membrane by vacuuming.

The individual gas permeabilities were evaluated by using Eq. (1).

$$p = \left(\frac{273}{76}\right)\left(\frac{V}{A}\right)\left(\frac{1}{273+T}\right)\left(\frac{l}{\Delta P}\right)\left(\frac{dP}{dT}\right) \quad (1)$$

Where P is the permeability of composite membrane (1 Barrer= 10^{-10} cm^3 (STP) cm/(cm^2 s cmHg)), dP/dT is the pressure gradient during time t in a steady state (torr/s), T is the operating temperature (°C), A is the membrane area pressure differences across the membrane, l is the thickness of composite membrane (cm), and ΔP is the pressure difference between the upper and lower sides. For comparison purposes, the separation factor, α, is determined by rationing the individual permeation rates.

When a mixture of gases is separated, the ideal separation factor for components is defined as the ratio of permeability of each component as follows, Eq. (2) [Leroux et al., 1994].

$$\alpha_{A/B}=P_A/P_B \quad (2)$$

4. Characterizations

The morphologies of polymerized PPy were analyzed by using scanning electron microscopy (SEM). The polymerized films were characterized by FT-IR, wide-angle X-ray diffraction (WAXD) used to characterize the d spacing. Thermogravimetry (TGA) was carried out on a thermogravimetric analyzer, using high-purity nitrogen as purging gas.

RESULTS AND DISCUSSION

1. The Effect of Gas Permeability and Selectivity with Preparation Parameters

As a first experiment, the thickness of polymerized PPy film was examined about the effect on the gas permeation properties. Polymerization time increased gradually because the polymerization time was related with the thickness of PPy film. During the experiments, $FeCl_3$ concentration (0.2 M) and pyrrole concentration (0.2 M) were kept constant. A total thickness of the prepared flat PPy/PDMS composite membrane was about 280 μm. The thickness of PPy film as selective layer was formed about between 100 and 600

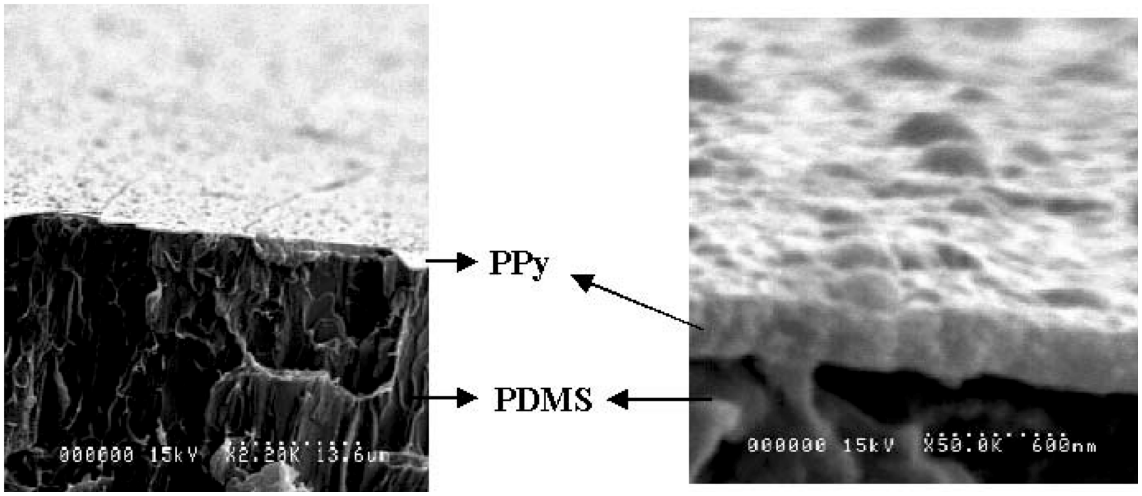

Fig. 1. The SEM image of flat polypyrrole/PDMS composite membrane after polymerization for 30 min.

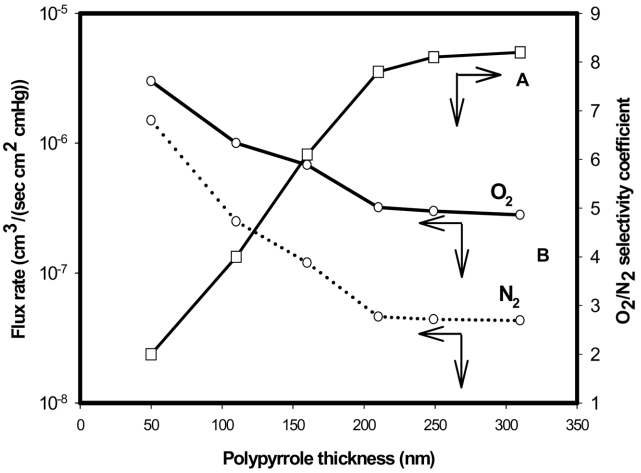

Fig. 2. Effect of polypyrrole film thickness of composite membrane on the O_2/N_2 selectivity coefficient (A) and the O_2 and N_2 permeability coefficient (B). free-standing films.

nm according to polymerization time (Fig. 1).

Gas permeation properties by thickness of PPy film are shown in Fig. 2(A) and (B). Fig. 2(A) shows the film thickness dependence of the apparent permeation rate (P/L) of oxygen. Also, Fig. 2(B) shows ideal selectivity for oxygen to nitrogen in PPy films deposited on the PDMS. PDMS itself is permselective to gases; the selectivity of pure gas permeates of N_2 and O_2 through PDMS film was 2.0, which compares very well to that published in the open literate [Robeson, 1991]. As shown in Fig. 2(B) the oxygen permeation rate started to decrease with increasing thickness of PPy film, and simultaneously the selectivity (α) started to increase. The gas selectivity showed dramatic changes at a film thickness of about 180 nm and was maintained changelessly at above that thickness. When the PPy/PDMS composite membrane is thin (e.g., below 100 nm), α_{O_2/N_2} is essentially at the permeability of PDMS value (2.0). This behavior indicates that polymerized PPy film formed a larger number of defects and/or pinholes. Increasing of PPy thickness reduces those defects, and finally homogeneous pinhole-free thin films are formed. The maximum selectivity coefficient value achieved, α_{O_2/N_2}=8.2, is identical to the selectivity coefficient obtained by Martin et al. [1997] for thin polypyrrole. These data show that free-standing membrane with thickness greater than 180 nm are essentially defect free.

Base on the above observations, the PPy film used in these investigations had thickness between 150-300 nm thicknesses on the PDMS membrane to observe gas permeation properties. Also, preliminary experiments were carried out to prepare composite membrane at various polymerization rates, maintaining the "optimum" polypyrrole thickness, and the best conditions were chosen to give the highest selectivity of gas pairs in the resulting PPy/PDMS composite membrane.

2. The Effect of Gas Permeation Properties with Polymerization Rates

To elucidate the polymerization rate effect on the membrane performance, several experiments were performed at different oxidizing agent concentration. We have since discovered that if the rate of pyrrole polymerization is decreased, polypyrrole films with a dense morphology can be obtained. The key feature of the synthetic method used here is the addition of ferrous chloride ($FeCl_2$) to the ferric chloride ($FeCl_3$) base polymerization solution. Fe^{2+} was added to slow the rate of polymerization down in order to obtain a dense polypyrrole film. Visual and electro microscopic examination of the films during synthesis showed that the rate of polymerization was, indeed, slower than when Fe^{3+} was used [Kesting, 1985; Kuwabata and Martin, 1994; Kesting and Fritzsche, 1993].

Kuwabata [Kuwabata and Martin, 1994] has shown that the rate of PPy polymerization is determined by the rate of initial electron transfer reaction.

$$Py+Fe^{3+/2+} \rightarrow Py^{\cdot+}+Fe^{2+}$$

Where Py is the neutral polypyrrole monomer and $Py^{\cdot+}$ is the corresponding radical cation. The rate of polymerization can, therefore, be varied by varying the initial concentration of Py and addition of ferrous chloride ($FeCl_2$) to the ferric chloride ($FeCl_3$) base polymerization solution in the polymerization solution used to synthesize the polymer. In this section have used this approach to prepare a series of PPy samples that were polymerized at various polymerization rates. The initial Fe^{3+}/Fe^{2+} and Py concentrations used to synthesize our PPy samples are shown in Table 1. Note that the initial ration oxidation agent (Fe^{3+}/Fe^{2+})/PPy was 10 : 1. However, the ferrous chloride ($FeCl_2$) concentrations were varied by over an order of magnitude. As indicated in Table 1, the polymer samples are identified by the notation PPy_x, where x is the initial concentra-

Table 1. Concentration used to synthesize the various polypyrrole samples.

Sample designation	$[Fe^{3+}]$ (M)	$[Fe^{2+}]$ (M)	[Pyrrole] (M)
PPy_2	1.0	2.0	0.1
PPy_1	1.0	1.0	0.1
$PPy_{0.5}$	1.0	0.5	0.1
$PPy_{0.25}$	1.0	0.25	0.1
$PPy_{0.13}$	1.0	0.13	0.1
$PPy_{0.06}$	1.0	0.06	0.1

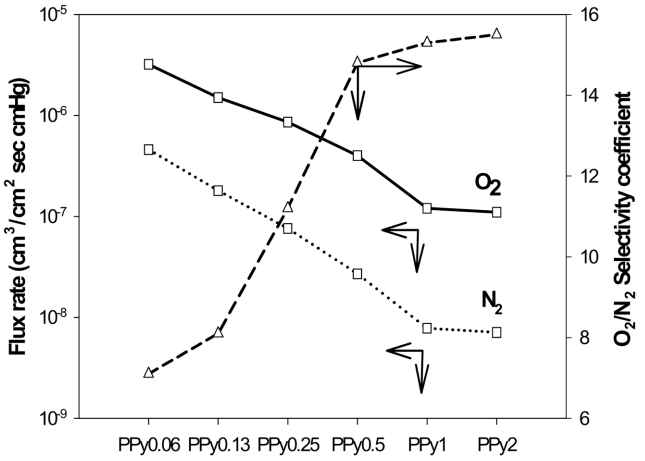

Fig. 3. Effect of polypyrrole film thickness of composite membrane on the O_2/N_2 selectivity coefficient and the O_2 and N_2 permeability coefficient by the rate of polymerizations decrease.

tion of Fe^{2+} used in the polymerization solution. High values of x indicate that the samples were polymerized at a relatively lower rate. Polymerization was allowed to proceed for 1.0 h. Additional polymer was not obtained at longer polymerization times.

Permeability obtained for these experiments is given in Fig. 3 and the corresponding selectivity change at these conditions is plotted in Fig. 3. Analogous selectivity and permeability coefficient versus polymerization rates were obtained for the composite membranes that yielded films thickness of 240 nm 25 nm of the polypyrrole layer coating on the PDMS support membrane surface. PPy/PDMS composite membrane showed that gas transport selectivity improved dramatically after the rate of polymerization went down (increased with the concentration of ferrous chloride). Obtained permeability and selectivity for these experiments are given in Fig. 3. For example, for PPy_2, compared with the polymerized membrane for $PPy_{0.06}$, the O_2 permeability coefficient is nearly 30 times lower than that for PPy_2, while the P_{O_2}/P_{N_2} selectivity of former membrane is 218% higher than of the latter membrane. Also, the N_2 permeability is 57 times lower than that of polymerized membrane for PPy_2; the best performance of the PPy/PDMS composite membrane shows O_2/N_2 selectivity of 14.8 and permeability of 4×10^{-7} cm^3/cm^2 sec cmHg. In comparison with high polymerization rate, the permeability values of PPy/PDMS composite membrane decrease slightly with decreasing rate of polymerization, and significant improvement on the gas selectivity was observed. Possible reason for this change in permeability and selectivity was explained by the fact that, since the rate of polymerization decreased including ferrous chloride, the possibility of forming pinhole diminishes or leads to denser structures.

3. FT-IR with Polymerization Rates

An IR spectrum for PPy with polymerization rate is shown in Fig. 4. To identify Py and PPy, the spectra were obtained of Py in a KBr tab and PPy [Janse et al., 1988]. The most intense bands in the PPy spectrum are 1,560 cm^{-1} (2,5-substituted PPy); 1,051 cm^{-1} (C-–H vibration of 2,5-substituted PPy); 922 and 738 cm^{-1} (C-H deformation of 2,5 substituted PPy) and 1,099 cm^{-1} (C-O asymmetrical stretching) (Fig. 4). These results indicate that a non-stoichiometric ratio of oxidant concentration to product yield was obtained when the reaction was PPy monomer and oxidant agents, and that the polymer consists of carbonyl and hydroxyl groups. Furthermore, it appears that the sorbed Py is polymerized when the membrane is exposed to ambient air and Fe^{2+} is oxidized to Fe^{3+}. In this case, the reaction rate would depend on the Fe^{2+} to Fe^{3+} oxidation rate and, hence, is slower relative to that seen in Fig. 4 (influence of O_2 on the polymerization rate). These values obtained for PPy are well matched with the reported value for PPy [Kesting and Fritzsche, 1993]. According to the spectrum of PPy, PPy identifying bands are 738 and 922 cm^{-1} (CH). In the spectrum of PPy membranes, we can see the bands attributed to PPy (1,569 cm^{-1} and 918 cm^{-1}) and those to PPy (738 cm^{-1}). These spectra show a featureless absorption tail at energies above 1,600 cm^{-1} and a series of bands below 1,600 cm^{-1}. The featureless tail is due to free-carrier absorption and is a unique signature of the conductive state.

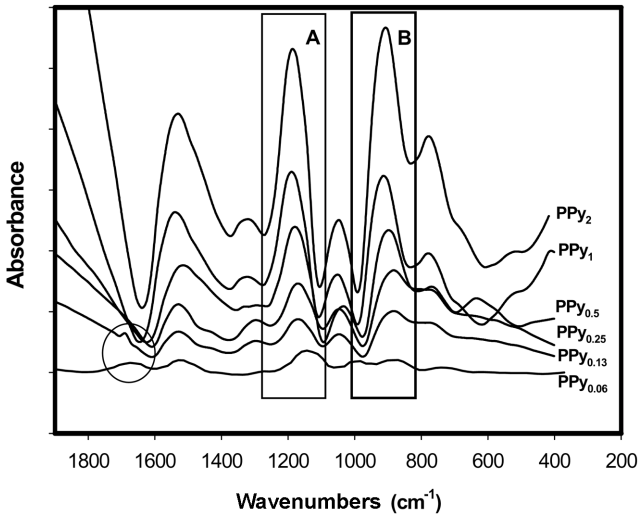

Fig. 4. FT-IR spectra of PPy film after polymerization by interfacial methods and the spectrum of PPy with the rate of polymerization.

In accordance with Tian and Zeribis nomenclature [1990], the so-called "doping-induced bands" (1,169 and 897 cm^{-1}) blue-shift upon conversion of fully oxidized PPy_2 and PPy_1 to a partially oxidized form (1,180 and 914 cm^{-1}). These indicate that base treatment yields an oxidized polypyrrole. Also, FT-IR spectra for $PPy_{0.06}$ and $PPy_{0.13}$ show a weak band at 1,705 cm^{-1}. This band has been observed in oxygen-oxidized and has been attributed to carbonyl. Fig. 4 shows that the intensity of this band decreases as the concentration of ferrous chloride used to synthesize the polymer decreases. Thus, the FT-IR data indicate that carbonyl is present in this PPy sample. As shown in Fig. 3, the gas permeation test of PPy/PDMS composite membrane showed that the gas permeability was dependent on the rate of polymerization. Gas permeation properties of gas membrane in conducting polymers including PPy are highly dependent upon the structural order. This morphology change led to a decrease in excess free volume of polymerized PPy film and to closer polymer packing.

The intrachain component is damaged by conformational and chemical defects within the structure of a polymer chain. PPy chains are intrinsically planar and linear except when defects are present within the chains [Demousiter-Champangne et al., 1999; Devlaux et al., 2000; Cuenot et al., 2000; Graham, 1866]. Conformational defects such as 2-2' coupling with non-regular 180° rotation (kink) of the alternating pyrrole unit break the planarity and linearity of the PPy chain and reduce the extent of π-orbital overlaps. Chemical defects such as 2-3' or 2-4' coupling and non-aromatic bonding break the π-conjugation as well as the planarity and linearity of a PPy chain. Overoxidation during the polymerization step is reported to introduce carbonyl or hydroxyls group into PPy chains, which shorten the conjugation length of the PPy chain, reducing the intrachain mobility [Mitchell et al., 1987].

The decrease in gas permeation of polymerized PPy film was contributed by polymer chain distribution. It was proposed that the decrease in gas permeation rate might be due to the polymer chain distribution by the rate of polymerization, which reduced with decreasing the rate of polymerization. In this study, conformational changes of a PPy chain induced by interaction with decreasing the rate of polymerization are expected to be a strong factor influencing intrachain mobility. These results indicate that denser PPy interchain polymer packing was formed by decreasing the rate of poly-

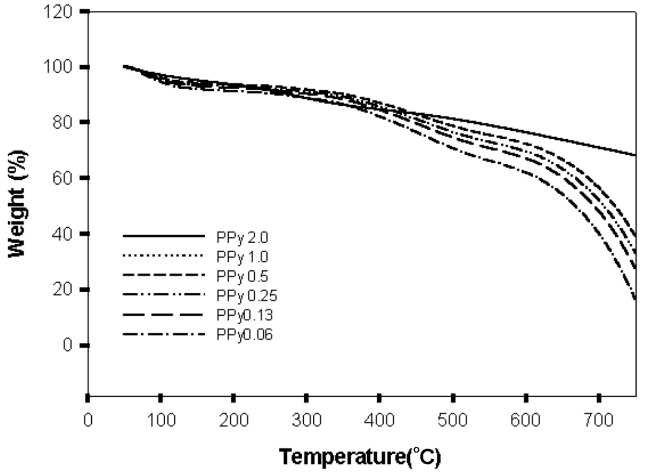

Fig. 5. TGA curves (under nitrogen flow) of PPy with the rate of polymerization.

merization and, then, led to the decrease in permeability and the increase in selectivity ratio of oxygen to nitrogen. For the high polymerization rate, the gas permeability increase and the selectivity decrease because of the intrachain mobility enhances by presence of defects such as 2-3' or 2-4' coupling and non-aromatic bonding break the planarity and linearity of a PPy chain. Therefore, the obtained high gas selectivity and lower permeation rate is due to the slower processes of Fe^{2+} oxidation and PPy polymerization.

4. Thermal Stability of PPy with the Rate of Polymerization

Fig. 5 presents the TGA curves of PPy with the rate of polymerization. The quite good thermal stability of pristine PPy is confirmed by the TGA study. It is theoretically possible to predict the thermal stability of any polymer by a group increment calculation [Henis et al., 1981]. We tried to apply this approach to PPy and the results were the following: maximum decomposition rate expected at 527 °C and the char residue at 750 °C expected to be 64.6±2.3 wt.%. Maximum decomposition rate is considered the temperature at which the weight loss up to 750 °C reached 50% of its total value, and for PPy this temperature was 527 °C. The total weight loss at 750 °C is only 30% of the initial weight; thus the char residue is 70% in good agreement with the theoretical value of 64.6%. Furthermore, if the total weight loss at 750 °C is 30%, the experimental temperature at which the weight loss is 15% is at about 515 °C, again in good agreement with the theoretical prediction of 527 °C. Fig. 5 also shows the completely different thermal behaviors of PPy with the rate of polymerization. For high rate of polymerization, the weight loss starts even at 50 °C and increases rapidly up to 225 °C; then the weight loss rate changes but continues linearly to 750 °C. Thus, we can distinguish two stages: the first, up to 225 °C, where the most volatile oxidized fraction is lost and then we have a second stage where the residual material is practically non-oxidized PPy, which in fact decomposes at a rate somewhat similar to the lower rate of polymerization (the slopes of the two curves run now quite parallel). From the TGA of Fig. 5 data we can even estimate the degree of oxidation of our polymerized PPy sample. In fact the initial weight loss from 50 to 250 °C involves a weight loss of the mentioned amount. The rate of weight loss then seems to accelerate a little and in general we can affirm that under an inert atmosphere PPy at high rate of polymerization (PPy_2 and PPy_1) appears to be less stable than its prepared PPy at lower rate of polymerization ($PPy_{0.06}$ and $PPy_{0.13}$). On the other hand, it was proposed that denser polymer packing was formed by decrease of the rate of polymerization.

5. Wide Angle X-ray Diffraction (WAXD) with the Rate of Polymerization

According to previous results, the various rates of polymerizations obviously involve a large range of permeability coefficients. Moreover, it provides an interesting increase in selectivity from 7.1 for $PPy_{0.06}$ to 15.5 for PPy_2. At this point of the study, we can presume that this permeability coefficient decrease is due to an increase in the density of the interchain in PPy film after lowering the rate of polymerization. There is doubt in that Ficks laws do not seem to explain the results for the rate of polymerization. We should find another material that may take into account physical interactions of permeation gases in the polymer. The WAXD method has been used to determine the interchain distance in amorphous polymer by measuring the maximum intensity in the amorphous scattering region [Lee et al., 1999].

WAXD patterns with the rate of polymerization in Fig. 6 prove that the PPy sample is semi-amorphous. Peaks at around 20 degree are well indexed to reflections of a cubic system with the cell parameter a=8.35 Å, respectively [Demoustier-Champange et al., 1999].

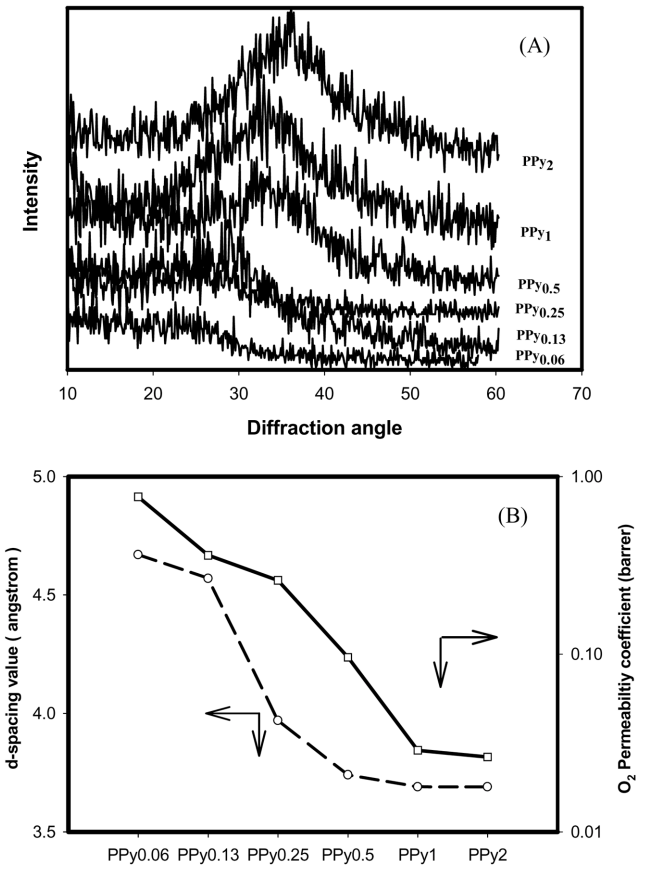

Fig. 6. (A) XRD patterns of PPy film with the rate of polymerization. (B) d spacing changes and oxygen gas Permeability coefficient of PPy/PDMS composite membrane with the rate of polymerizations. Thickness of Each PPy samples was 240 ±20 nm.

If the material is crystalline in nature, the peak from the X-ray diffraction is sharp and the intensity is strong. However, when the material is amorphous, the peak is rather broad. In the case of the present PPy, as can be seen in the WAXD patterns in Fig. 6A PPy is regarded as a rather amorphous material. However, the WAXD pattern of an amorphous polymer is typically dominated by one broad peak associated with the center-to-center chain distance or d spacing. d spacing values are calculated from Bragg's equation, $n\lambda=2d \sin\theta$ where θ is the angle for a peak in the patterns. Here, 2θ at the maximum intensity appearing at around 20^{o} was used to calculate the d spacing, which was representative of the average openness degree within a material.

Changes in d spacing with the rate of polymerization are shown in Fig. 6B. The d spacing of the present $PPy_{0.06}$ film is 4.62 Å, which is much high than the kinetic diameter of O_2. As the rate of polymerization increases, the d spacing decrease reaches 3.6 Å, which is close to the value of doped PPy film (3.67 Å). If we compare the kinetic diameter of permeating gases, 3.46 Å for O_2 and 3.64 Å for N_2, it is clear that a membrane having a d spacing between two values is regarded as an ideal separating membrane with unlimited selectivity. As the d spacing decreases, the oxygen and nitrogen permeability coefficients concurrently decrease. Also, Fig. 6B shows the relationship between the permeability coefficients and the molecular diameter of permeants gases for PPy/PDMS composite membrane. Kinetic molecular diameter is defined as the intermolecular distance of closest approach for the same two molecules colliding with zero initial kinetic energy and is based on Lennard-Jones potential theory [Jasne et al., 1988]. Kinetic molecular diameters of the gases used are O_2 (3.46 Å) and N_2 (3.64 Å). The gas permeability coefficients were shown to depend on the molecular diameter of gases as shown in Fig. 6B. This behavior suggests that the permeability is distinguished by the size and shape of gas molecules; in other words, the permeability is controlled by the diffusion coefficient, reflecting the packed structure of the PPy film. Therefore, in this study, the d spacing of the PPy film decreased from 4.89 to 3.67 Å by decreasing the rate of polymerization. As lowering of the rate of polymerization continued, the d spacing decreased, resulting in a dramatic increase in selectivity of the PPy composite membrane. The increase of diffusion selectivity is attributed to the change of d spacing caused by the rate of polymerization.

CONCLUSIONS

The fabrication of high-flux composite membranes requires deposition of an ultrathin, discriminating layer on a highly permeable support. In this study, we show that different morphology of PPys films was obtained by controlling polymerization rate and more dense films were formed at low polymerization rate. The lower the rate of PPy polymerizations, the more the permeability of a PPy/PDMS membrane decreased while selectivity slightly increased, because of the changes in morphology of PPy. The d spacing of the PPy film decreased from 4.89 to 3.67 Å by decrease of the rate of PPy polymerization. As lowering of the rate of polymerization continued, the d spacing decreased, resulting in a dramatic increase in selectivity of a PPy composite membrane. The highest selectivity value of composite membrane that was prepared by interfacial polymerization was O_2/N_2=17.2 and permeability for O_2 was 40.2 barrer.

REFERENCES

Abelson, P. H., "Synthesis Membrane," *Science*, **244**, 1421 (1989).
Cuenot, S., Demoustier-Champagne, S. and Nysten, B., "Elastic Modulus of Polypyrrole Nanotubes," *Phys. Rev. B.*, **85**, 1690 (2000).
Delvaux, M., Duchet, J., Stavaux, P.-Y., Legras, R. and Demoustier-Champagne, S., "Chemical and Electrochemical Synthesis of Polyaniline Micro- and Nano-tubules," *Synth. Met.*, **113**, 275 (2000).
Demoustier-Champagne, S. and Stavaux, P.-Y., "Effect of Electrolyte Concentration and Nature on the Morphology and the Electrical Properties of Electropolymerized Polypyrrole Nanotubules," *Chem. Mater.*, **11**, 829 (1999).
Haggin, J., "Membranes Technology has Achieved Success, yet Lags Potential," *Chem. Eng. News*, **68**, 22 (1990).
Henis, J. M. S. and Tripodi, M. K., "Novel Approach to Gas Separations using Composite Hollow Fiber Membranes," *Sep. Sci. Technol.*, **15**, 1059 (1980).
Henis, J. M. S. and Tripodi, M. K., "Composite Hollow Fiber Membranes for Gas Separation: The Resistance Model Approach," *J. Membr. Sci.*, **8**, 233 (1981).
Jasne, R. and Mark, H. F., *Encyclopedia of Polymer Science and Technology*, Wiley, New York, **13** (1988).
Kesting, R. E. and Fritzsche, A. K., *Polymeric Gas Separation Membranes*, John Wiley & Sons, New York (1993).
Kesting, R. E., *Synthetic Polymeric Membranes; A Structural Perspective*, John Wiley & Sons, New York (1985).
Kuwabata, S. and Martin, C. R., "Investigation of the Gas-transport Properties of Polyaniline," *J. Membr. Sci*., **91**, 112 (1994).
Lee, Y. M., Ha, S. Y., Lee Y. K., Suh, D. H. and Hong, S. Y., "Gas Separation through Conductive Polymer Membranes. 2. Polyaniline Membranes with High Oxygen Selectivity," *Ind. Eng. Chem. Res.*, **38**, 1917 (1999).
Leroux, J. and Paul, D. D. R., "Modification of Asymmetric Polysulfone Membranes by Mild Surface Fluorination Part I. Transport Properties," *J. Membr. Sci.*, **94**, 121 (1994).
Martin, C. R., Parthasarathy, R. V. and Menon, V. P., "Unusual Gas-Transport Selectivity in a Partially Oxidized Form of the Conductive Polymer Polypyrrole," *Chem. Mater.*, **9**, 560 (1997).
Mitchell, G. R. and Geri, A., "Molecular Organisation of Electrochemically Prepared Conducting Polypyrrole Films," *J. Phys. D: Appl. Phys.*, **20**, 1346 (1987).
Robeson, L. M., "Correlation of Separation Factor Versus Permeability for Polymeric Membranes," *J. Membr. Sci*., **62**, 165 (1991).
Spillman, R. W., "Economics of Gas Separation Membrane," *Chem. Eng. Prog*., **85**, 41 (1989).
Tian, G. and Zerbi, G., "Lattice Dynamics and Vibrational Spectra of Polypyrrole," *J. Chem. Phys*., **92**, 3886 (1990).